Numerical study on the performance of improved masonry-to-timber connections in traditional masonry buildings

Ana S. Araújo[1], Daniel V. Oliveira[2], Paulo B. Lourenço[3]

ABSTRACT

This paper deals with a numerical study on the structural performance of masonry-to-timber connections in ancient buildings. The work is supported on an experimental campaign carried out at University of Minho, which aims at characterizing a strengthening solution based on the use of injected anchors for the improvement of the connection between masonry and timber frame walls. The numerical study resorts to a detailed 3D finite element model, which reproduces the experimental test setup and procedure. The modelling approach adopted allows an accurate characterization of the behaviour of all structural elements, in terms of stress field and displacement distribution. The 3D model was validated against the available experimental results, which was then used to perform parametric analyses in order to evaluate the influence of key parameters. Finally, simplified analytical approaches to estimate the strength capacity of injected anchors on masonry are presented and discussed.

Keywords: masonry, injection anchors, tensile strength, numerical analysis.

1. INTRODUCTION

Most of the Portuguese traditional buildings are made of unreinforced stone masonry walls and flexible timber diaphragms, with the exception of a few cases in which the timber floors and roofs provide efficient in-plane stiffness [1]. Given its widespread presence worldwide, recent seismic events have emphasized the great vulnerability of the majority of these masonry buildings, mostly due to the lack of effective connections between elements [2]. Evidence from the recent 2011 New Zealand earthquake, among many others, confirmed that out-of-plane wall collapse was one of the main collapse mechanisms observed in masonry buildings, which is strongly dependent on the connection quality [3]. When not properly connected to the roof, floors and perpendicular walls, a masonry wall can easily become unstable and collapse out-of-plane, compromising in this manner the global capacity of the structure. When walls are seismically excited in their plane, the excitation has generally a small amplification because of the large stiffness and low natural period. On the contrary, walls subjected out-of-plane present a quite large seismic amplification, due to their low stiffness and high natural period.

Hence, the structural performance of traditional masonry buildings to seismic actions depends on their capability to redistribute the horizontal loads between the vertical elements, which allows exploring in-plane strength of the walls at its maximum and preventing local out-of-plane mechanisms.

[1] PhD Student, ISISE, University of Minho, Department of Civil Engineering, Azurém, 4800-058 Guimarães, Portugal. Phone: +351 253 517 210, fax: +351 253 510 217, E-mail: ana.araujo@civil.uminho.pt

[2] Associate Professor, ISISE, University of Minho, Department of Civil Engineering, Azurém, 4800-058 Guimarães, Portugal. Phone: +351 253 510 247, fax: +351 253 510 217, E-mail: danvco@civil.uminho.pt

[3] Professor, ISISE, University of Minho, Department of Civil Engineering, Azurém, 4800-058 Guimarães, Portugal. Phone: +351 253 510 209, fax: +351 253 510 217, E-mail: pbl@civil.uminho.pt

Assuming that the quality and state of conservation of vertical elements is good and that the horizontal elements have enough stiffness to redistribute horizontal actions, the building global performance is greatly influenced by the effectiveness of the connections between vertical elements and between vertical and horizontal elements. If these connections are ineffective, a global behaviour cannot be achieved and the building may collapse under the effect of low seismic excitations by developing local mechanisms.

Bearing in mind the typical structural organization of traditional masonry buildings, the capability of the structures to redistribute horizontal loads depends on the connection between orthogonal walls, the flexibility of the diaphragms and their connection to the masonry walls [4]. The combination of the referred aspects provides the so called “box behaviour” to the building, which usually leads to a good performance of the structure when subjected to horizontal actions [5], [6].

The seismic response of masonry buildings to past earthquakes showed that the strengthening of connections between structural components (walls and floors) can enhance the global seismic performance in a significant way. Senaldi et al. [3] present some successful examples of retrofitted masonry buildings that survived the recent 2011 NZ earthquake without suffering major damage. It was observed that the strengthening of connections using anchoring systems and the insertion of steel tie rods at floor and roof levels proved to be effective in preventing local out-of-plane collapse of walls under seismic events.

The performance of connections in masonry buildings has been studied by a few authors, either evaluating the behaviour of a single connection or analysing the effect of connections on the global behaviour of a building. For example, the use of steel to strengthen ancient masonry buildings has been observed since the 1920s [7]. On the other hand, a dissipative device to improve the connection of perpendicular walls was recently proposed by Paganoni and D’Ayala [8]. Some examples of traditional and innovative strengthening solutions for connections can be found in [2], [9], [10].

Injected anchors are particularly well suited to repair and strengthen ancient masonry buildings as they allow for an effective connection between perpendicular walls, thus avoiding overturning of walls excited out-of-plane and activating the relatively stable in-plane behaviour of adjacent walls.

However, there is an evident lack of experimental and numerical studies in this field, which are necessary for a clear characterization of the structural behaviour of these connections. Thus, this paper presents a detailed numerical study based on the use of injected anchors for the strengthening of masonry-to-timber connections. In a first step, the numerical model was validated against existing experimental results obtained at University of Minho. Subsequently, parametric analyses were then carried out aiming at evaluating the influence of key influencing parameters on the behaviour of the strengthened connection. Finally, analytical relationships to estimate the maximum force that an injected anchor in a masonry wall is able to carry were revised and compared against the numerical and experimental results.

2. EXPERIMENTAL BEHAVIOUR OF ANCHORING SYSTEMS

2.1 Potential failure modes

The anchoring system considered here consists of a steel element inserted in a core made in a masonry wall filled with grout. The load transfer between the steel element and the surrounding masonry comprises two interfaces: the outer intersection between masonry and grout, and the inner intersection between grout and the steel element. Experimental results indicate that the main factor limiting the capacity of the anchoring system is usually not the failure of steel or the steel/grout interface, but rather the somehow reduced shear and tensile strength of the masonry substrate to which the anchor is injected.

Still, the possible failure modes experimentally identified for injected anchors in masonry are similar to the ones found for anchors in concrete [11–15]. When subjected to tensile loading, injected anchors in masonry may exhibit the following failure mechanisms (see also Figure 1):

- Steel tensile failure: the anchor is loaded until the yielding of steel (Figure 1a);
- Masonry cone failure: shear cone-like surface failure that occurs in the masonry with detachment of a small part of the wall around the anchoring system (see Figure 1b);
- Sliding failure along the outer interface: sliding of the anchoring system by failure at the masonry-grout interface (outer interface) with the disconnection of the anchoring system from the wall (see Figure 1c);
- Sliding failure along the inner interface: sliding of the steel anchor along the steel-grout interface (inner interface), involving local failure (see Figure 1d).

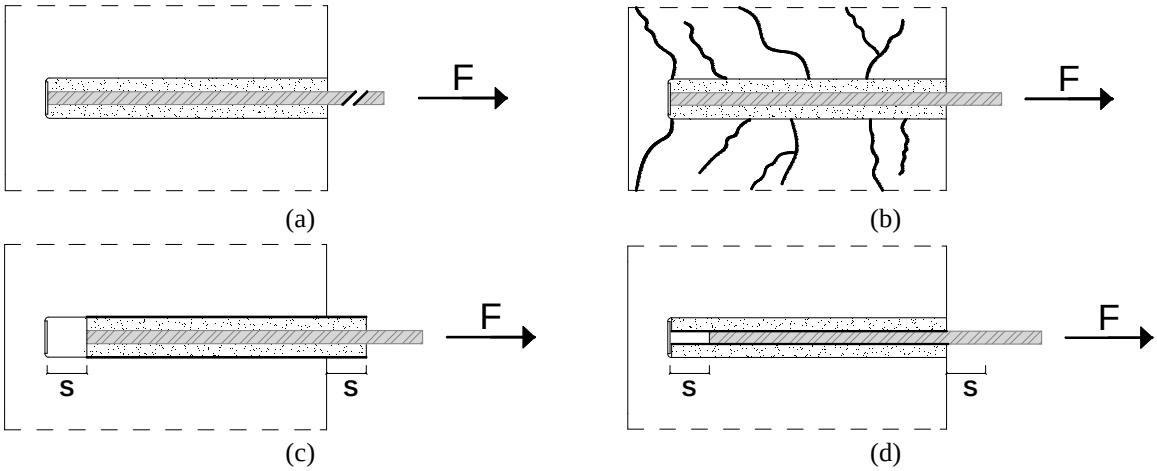

Figure 1 – Possible failure mechanisms in anchoring systems: (a) Steel failure; (b) Masonry cone failure; (c) Sliding failure along the outer interface; (d) Sliding failure along the inner interface.

Although the four individual failure mechanisms are possible, steel failure is rarely observed and takes place only in cases when the embedment depth and strength of the masonry are very high. A combination of two different failures was also observed experimentally [15], [17]. Usually, the masonry cone failure occurs with the presence of the cone formation simultaneously with sliding along the outer interface (also called bond failure).

2.2 Experimental tests carried out at UMinho

The design of injection anchors for masonry is a challenge due to the lack of codes and recommendations regarding the estimation of the strength capacity. Consequently, experimental campaigns aiming at studying the behaviour of injected anchors in both brick and stone masonry walls were carried out by a number of researchers [11–13], [16], [17].

The experimental work recently carried out at University of Minho on connections aimed at assessing the performance of masonry-to-timber connections, which are applicable to wall-to-wall connections representative of ancient buildings built after the 1755 Lisbon earthquake, strengthened with injected anchors. Figure 2 illustrates the strengthening solution adopted for the improvement of the connection between external and internal walls, consisting of two parallel Cintec® (www.cintec.com) anchors injected in the external masonry wall and connected to the internal wall by means of suitable steel plates. All steel is AISI Type 304 class 70 stainless. The main experimental results used in the numerical study are summarized here. Detailed information regarding the experimental campaign can be found elsewhere [22].

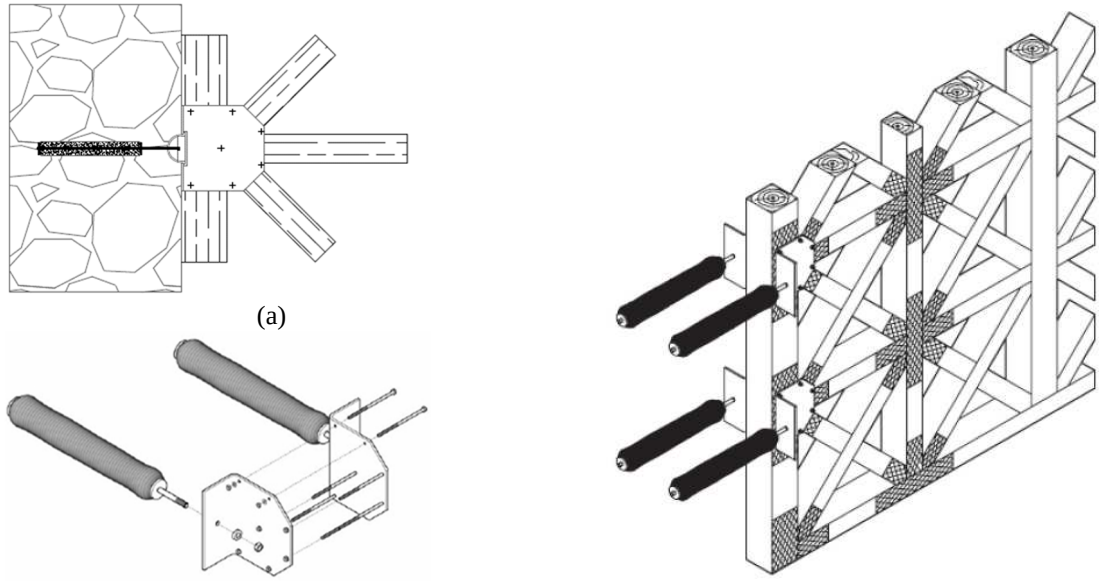

(a) (b) (c)

Figure 2 – Strengthening solution: (a) Elevation view of masonry section and detail of half-timbered perpendicular wall; (b) Detail of the strengthening system, with a pair of anchors; (c) Detail of one connection applied to a half-timbered wall [23].

The experimental campaign included the construction and testing of several real scale masonry walls in which Cintec® anchors were applied, see Figure 3. The walls were constructed with rubble limestone units and included the introduction of four pairs of parallel anchors in two levels. The 16 mm diameter steel bars were inserted into the wall through 50 mm diameter boreholes injected with a proprietary Cintec® grout (Presstec™), resulting in a two-anchor system with 280 mm distance between anchors. Monotonic and cyclic pull-out tests were performed in order to assess the performance of the anchoring system and to characterize its behaviour. The numerical study here focuses only on the analysis of the upper level anchorages, which are the ones tested first.

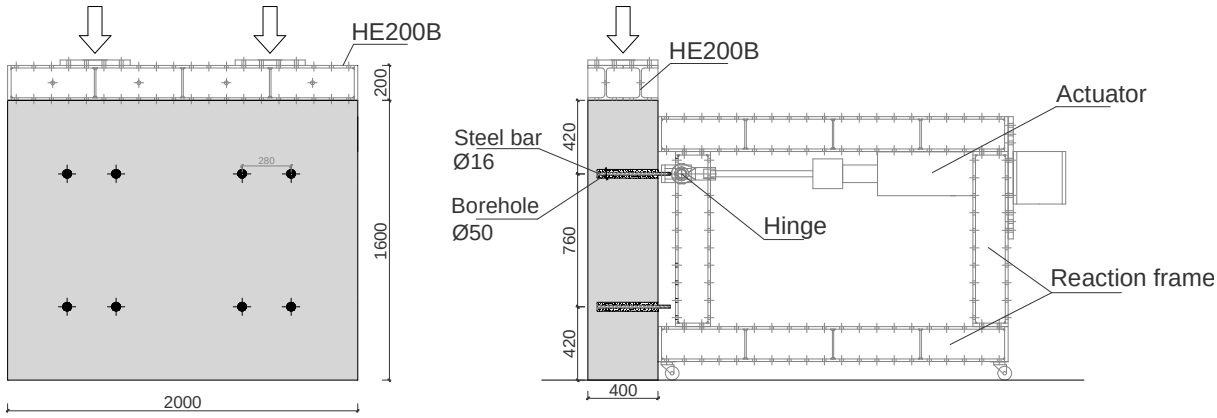

(a) (b)

Figure 3 – Specimen configuration (in millimetres): (a) Front view with location of anchors; (b) Cross section of wall and test set-up.

The experimental tests were carried out by the following described next. First, the vertical load was applied with two actuators designed to apply a constant compressive stress of 0.20 MPa to the masonry wall through the stiff metallic beams, in order to simulate the effect of dead load in the structure. Afterwards, each pair of anchors was subjected to horizontal monotonic or cyclic displacements until failure was reached. The out-of-plane displacements of the wall are limited by the

use of a self-balanced reaction frame. During the experimental campaign, several mechanical tests were carried out on stone, mortar and masonry specimens. The compressive tests carried out on six masonry prisms provided an average compressive strength of 1.74 MPa and an elastic modulus of 1.0 GPa. Further details are given in Moreira et al. [22].
The results from one monotonic and two cyclic experimental tests showed that the formation of a shear cone combined with sliding was the recurrent failure mode. The masonry cone failure is characterised by the formation of a roughly conical fracture surface radiating from the edge of the anchor. Note that the total displacement is a combination of the masonry shear cone formation with the relative displacement of the steel bar-grout (referred as inner interface) and grout-masonry (referred as outer interface) interfaces. The outcome obtained from the measuring LVDT´s was used for the definition of the global horizontal force-displacement curves for each test. Figure 4 illustrates the experimental envelope from the individual force displacement curves of three tests. The average maximum load equals 76.8 kN.

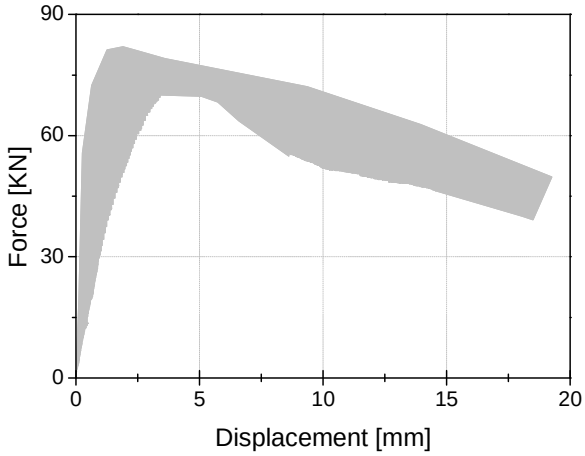

Figure 4 – Experimental envelope of three force-displacement curves.

3. NUMERICAL ANALYSIS

3.1 Numerical Model

A detailed 3D finite element model (FEM) was developed in DIANA 9.4 [24] aiming at an accurate simulation of the structural behaviour of the injected anchors. Three-dimensional volume elements were used for the mesh since an accurate stress distribution is relevant for a clear understanding of the stress field and of the structural behaviour, see Figure 5a. In order to simulate the behaviour of the different failure mechanisms, the model includes also interface elements around the steel bar (inner interface) and between the grout and the masonry (outer interface).
The mesh was defined aiming a compromise between accuracy and efficiency. Brick elements (CHX60, twenty nodes) are predominantly used for the mesh, although some tetrahedral elements (CTP45, fifteen nodes) were also adopted for the steel bars. For the simulation of the bond between different materials, tri-dimensional interface elements (CQ48I, eight nodes in each surface) were applied. Figure 5b illustrates the modelling strategy used for the numerical simulation of the anchoring system. All the elements include quadratic interpolation. The generated mesh includes 39,555 nodes and 9,441 elements. The discretization was refined in the surrounding areas of the anchors in order to provide reliable results, with acceptable computational efforts and time requirements.

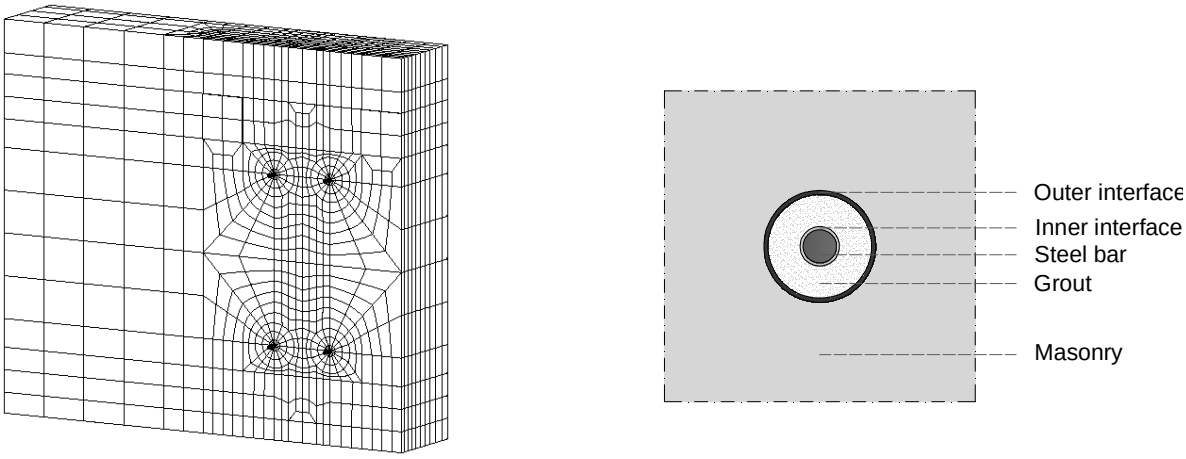

(a) (b)

Figure 5 – Numerical model: (a) Mesh; (b) Anchor modelling detail (fictitious thickness).

The model is fully restrained at the bottom as well as along the horizontal axis perpendicular to the façade on the two top areas of the wall in contact with the reaction frame, which reproduces the restraint provided by this apparatus.

Masonry was assumed as a homogeneous isotropic material with mean-value properties, which is a good compromise between accuracy and efficiency [25]. The value of the Young's modulus for masonry was based on the compression tests results performed on masonry prisms. The Poisson ratio was set equal to 0.20. The usual elastic modulus of steel was used. Regarding the physical and mechanical properties of the grout, information from the technical sheet was used. Table 1 provides the elastic properties adopted for the materials.

Table 1 – Properties of the materials

	E (GPa)	ν (-)	γ (Kg/m^3)
Masonry	1.0	0.2	1900
Steel bar	210	0.3	7850
Grout	30	0.2	2300
HE200 B profile	210	0.3	7850

Although injected anchors have been in use for many years on masonry, only a few studies focused the investigation of the behaviour of the bond between steel and grout or between grout and masonry. As the experimental campaign carried out did not include the mechanical characterization of the interfaces, the interface stiffness was defined according to the available literature. Here, studies in the field of concrete-steel bond behaviour in reinforced concrete were taken as an approximation. A range of values around 9-400 MPa/mm, depending on the bond conditions, has been indicated for the tangential stiffness of the inner interface according to investigations in this field [22–25].

A number of investigations on the behaviour of grout-masonry interfaces were performed considering different support materials. Bajer and Barnat [30] carried out experimental tests and numerical analyses for the study of the glue–concrete interface of bonded anchors under tensile load and a value around 500 MPa/mm was pointed out for the shear stiffness. The bond between grout and surrounding brick masonry was investigated by Gigla [15], providing values between 55 MPa/mm and 66 MPa/mm for the shear stiffness. Literature studies concerning unit-mortar interface on masonry (which can be also associated to the grout-masonry bond), as well as some expressions for its calculation, were also considered to estimate the interface parameters [27–30]. Thus, a range of values around 10-500 MPa/mm seems reasonable for the outer tangential stiffness. The usual elasticity equations relating

normal and tangential stiffness indicate that the normal stiffness is approximately twice the tangential one.

3.2 Non-linear Analysis and Model Validation

The experimental test procedure was followed for the numerical analysis, where the compressive vertical load was applied on the top of the metallic beam and an upper pair of anchors was loaded in tension by applying increasing horizontal displacements at its end.
A set of linear elastic analysis was carried out first in order to calibrate suitable interface stiffness values that best match the experimental curves in the linear range. These analyses proved that the values of the normal stiffness do not have a strong influence on the structural behaviour of the system and therefore were considered to be twice of the tangential one. This inverse fitting process resulted in the values presented in Table 2, which are within the range defined by literature. A comparison in terms of force-displacement between the experimental envelope and the numerical analysis result is given in Figure 6.

Table 2 – Interface Stiffness

Inner Interface		Outer Interface	
Tangential stiffness	Normal stiffness	Tangential stiffness	Normal stiffness
100	200	50	100

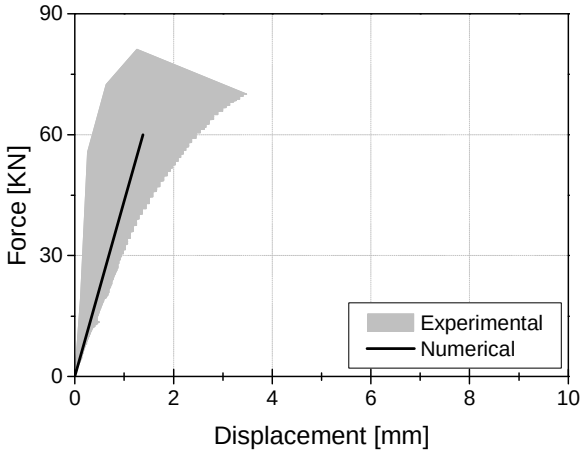

Figure 6 – Comparison between the experimental envelope and the linear numerical behaviour.

The non-linear behaviour of the masonry is modelled by adopting two constitutive models based on the total strain crack model: the total strain fixed crack model (FCM) and the total strain rotating crack model (RCM), both available in DIANA 9.4 [24]. In both models a crack is initiated when the maximum principal stress equals the tensile strength of the material and the initial orientation of the crack is normal to the maximum principal strain. In the fixed crack model the strain transformation matrix is fixed upon cracking and the crack plane is also fixed during the full analysis process. On the other hand, in the rotating crack model the crack direction rotates with the principal strain axes ensuring that the crack remains normal to the direction of the maximum principal strain. The rotating crack model is more flexible and allows a gradual correction of an initially mispredicted crack direction. In the fixed crack model, a shear retention factor has to be chosen for the definition of the shear behaviour, which leads to some stress built-up and locking. On the contrary, in the rotating crack model the shear stiffness is evaluated during the analysis and updated taking into account the current damage state [36]. It is expected that the structural behaviour of the model becomes highly dependent

on the shear behaviour of masonry. Therefore, both formulations were adopted and analysed, aiming at discussing the most suitable approach for this type of problems.
Most of the non-linearities are expected to concentrate in the masonry, since at the time masonry fails, steel and grout are most probably still in the linear range. As such, only masonry is considered with non-linear behaviour in the present model. Masonry is modelled using exponential softening in tension and a parabolic strain-stress relationship in compression, for both fixed and rotating formulations. While shear behaviour does not require the user definition within the rotating crack model, in the fixed crack model the post-cracked shear behaviour was modelled using a constant shear retention factor. The nonlinear properties for the masonry constitutive models definition were estimated based on recommendations from Lourenço [37], [38] and on the existing experimental results. The adopted values for the definition of the nonlinear constitutive models for masonry are summarized in Table 3. A Newton–Raphson iteration procedure was used with displacement control and an energy convergence criterion of 10^{-3}.

Table 3 – Non-linear parameters for the masonry

Compression		Tensile		Shear
f_c (MPa)	G_c (N/mm)	f_t (MPa)	G_t (N/mm)	β*
1.74	2.8	0.10	0.05	0.01

*Shear factor only for the fixed crack model

Figure 7 presents the force-displacement curves from the FCM and RCM and also the experimental envelope. The comparison of the numerical analyses (FCM and RCM) against the experimental envelope does not show significant differences concerning the linear behaviour and peak force, as expected. Although both numerical curves present a sudden decrease in load capacity just after the peak, the post-peak response exhibits considerable differences. The FCM formulation provides a continuously increase of the force after peak, which is not in agreement with experiments. In fact, the experimental post-peak envelope shows clearly a gradual force decrease with respect to displacement, which is well captured by the RCM formulation. This last approach provides a maximum force of 69 kN (90% of the mean experimental value) and an ultimate displacement of 15 mm.
Figure 7 shows clearly that the shear model can have a great influence on the post-peak behaviour of this type of structures, making the difference between a realistic structural modelling of the system and an incorrect overestimation of strength, even if the first peak is independent of the model. Still, and given this, the RCM will be used in the parametric analyses.

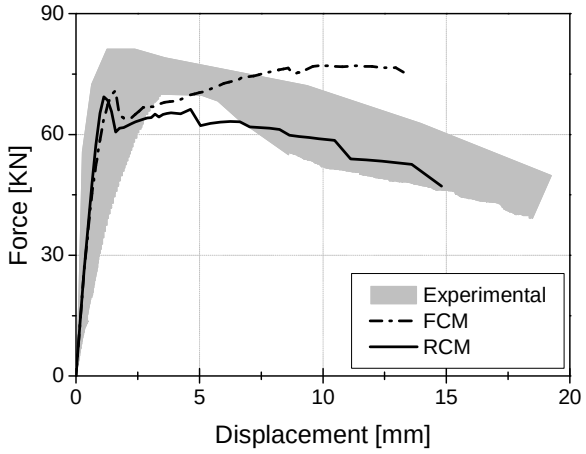

Figure 7 – Force-displacement curves for the RCM and FCM formulations and experimental envelope.

To further discuss the numerical behaviour, the maximum (tensile) principal strains are plotted and analysed as an indicator of damage. Figure 8 shows the maximum principal strains at peak load, for both constitutive laws. The distribution of damage is very similar for both models in the surrounding areas of the anchors, although it is more severe in the FCM. The top cross section shows damage along the anchors for the FCM while diagonal strain concentrations were found for the RCM. Despite the differences found in the level of damage for both analyses, the crack pattern at peak is very similar, being characterized by the formation of a shear cone on masonry, thus leading to a masonry cone failure with sliding trough the external interface.

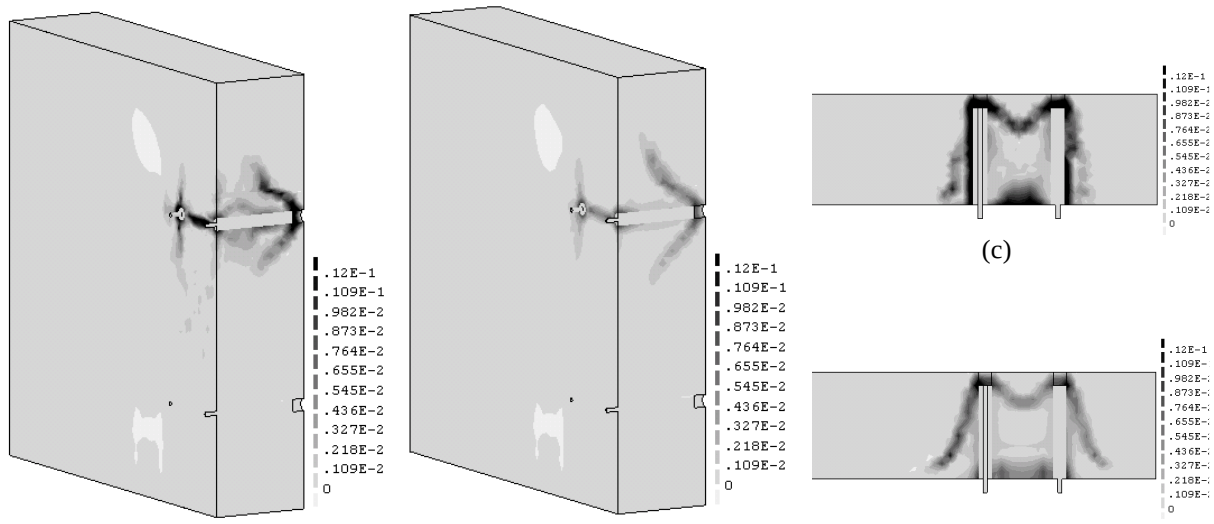

Figure 8 – Maximum principal strains depicted at vertical and horizontal cross sections for peak load: (a) FCM; (b) RCM; (c) FCM; (d) RCM.

4. PARAMETRIC STUDY

Experimental campaigns carried out on injected anchors in masonry showed that the primary factors affecting the performance of the anchoring system are the anchor diameter, the anchor embedment depth and the masonry tensile strength [12], although other parameters might influence the behaviour of the system as well. The study of the influence of all these parameters is almost impractical from an experimental point of view and therefore numerical investigations based on calibrated reliable models appear as an interesting alternative.

This section presents a parametric analysis of the anchoring system, where the following parameters of masonry were considered: (i) compressive strength; (ii) compressive fracture energy; (iii) tensile strength; (iv) tensile fracture energy; (v) pre-compression level. The purpose is to evaluate the variation on the structural response with respect to the reference model, varying each parameter from 50% to 200% of its initial value. Additionally, a few relevant geometric parameters were also varied.

4.1 Compressive strength and compressive fracture energy

Figure 9a depicts the reference model behaviour and the force-displacement curves obtained by varying the compressive strength. The 50% reduction of the initial compressive strength ($0.5f_{,ref}$) leads to a reduction on the peak load of around 10% in relation to the reference model, followed by a more pronounced post-peak degradation until failure. In contrast, the doubling of the compressive strength ($2.0f_{,ref}$) originates an important increase of the applied force, even if this is after a first peak. This means that the masonry compressive strength can be a relevant parameter in the anchoring system

behaviour. Regarding the compressive fracture energy variation, Figure 9b proves that this parameter does not influence much the initial behaviour of the system while for larger displacements some differences in the post-peak behaviour can be found.

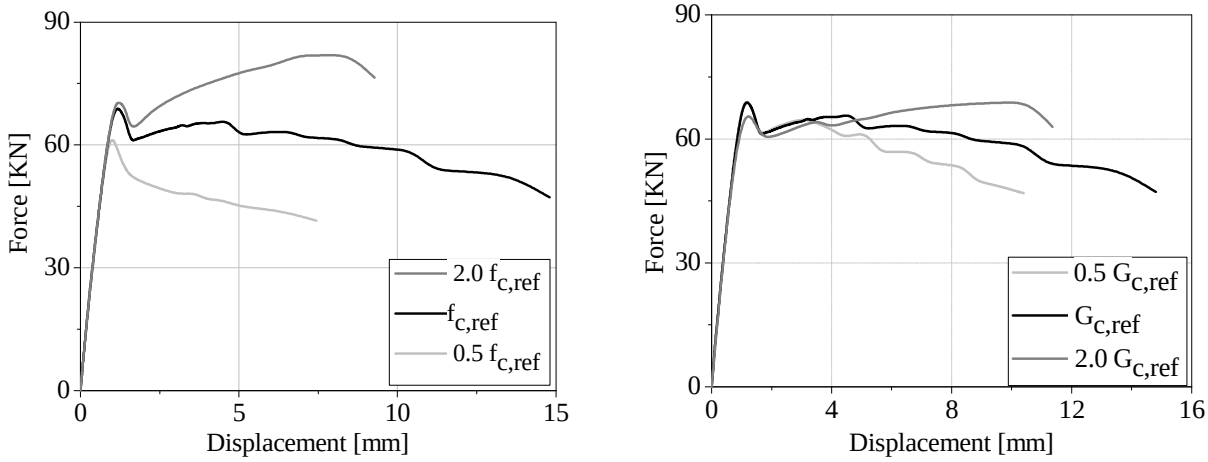

Figure 9 – Force-displacement curves of compressive non-linear parameters: (a) Strength; (b) Fracture energy.

4.2 Tensile strength and tensile fracture energy

The parametric analysis results of the tensile non-linear properties are plotted in Figure 10. As expected, the tensile parameters have a considerable influence on the global behaviour of the anchoring system. With respect to the analysis that adopts a reduction on the masonry tensile strength, the non-linear behaviour is activated for a lower value of applied force when compared to the reference model, even though it continues to increase up to 80kN, see Figure 10a. The fact that the corresponding fracture energy remains unchanged in face of the variation in the tensile strength value should be highlighted and can justify the high force capacity increase originated by the reduction of the tensile strength, visible in Figure 10a.

By increasing the tensile strength, the peak force also reaches a higher value when compared to the corresponding one from the reference model. However, in what concerns the post-peak behaviour the improvement is not so noteworthy. Indeed, the response of the $2.0f_{t,ref}$ model exhibits a more fragile behaviour since this model considers a tensile strength increase while keeping the fracture energy value unchanged. The tensile fracture energy sensitivity analysis confirmed the influence of this parameter on the peak load and the slight alteration on the post-peak behaviour of the structure.

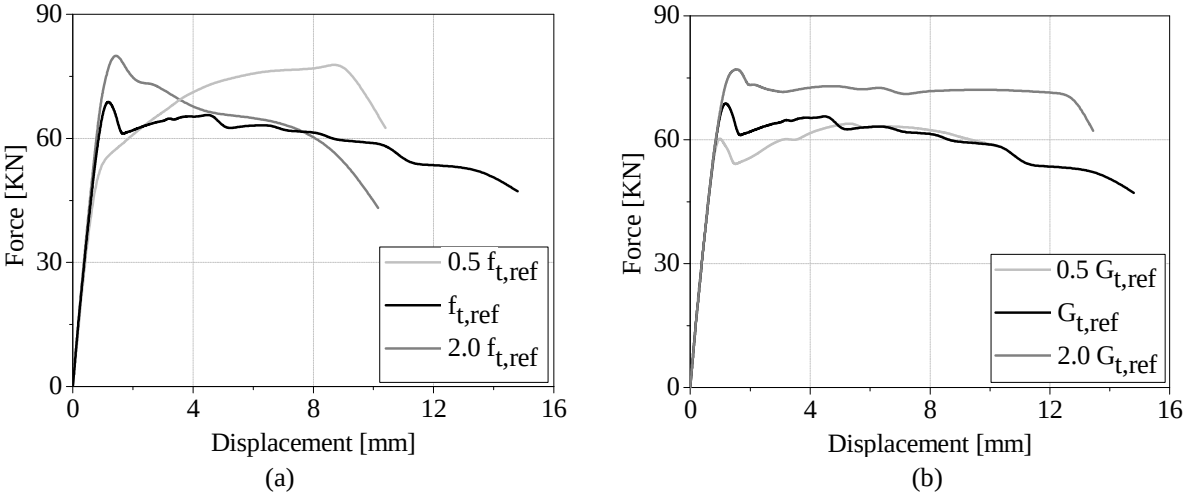

Figure 10 – Force-displacement curves of tensile non-linear parameters: (a) Strength; (b) Fracture energy.

4.3 Pre-compression level

The pre-compression level that the masonry wall is subjected to was decreased (0.10 MPa) and increased (0.40 MPa) two times the reference value. The results are depicted in Figure 11 in terms of global force-displacement curves. The pre-compression level has a significant influence on the maximum force that the anchoring system can carry. By decreasing the compressive stress on the wall, the peak force suffers a reduction of 14%. Likewise, the increasing of the level of pre-compression on the wall causes a 22% increase in the ultimate capacity of the structure. In both cases, the post-peak configuration is not very much affected. By the analysis of the damage, the failure mode is kept unchanged.

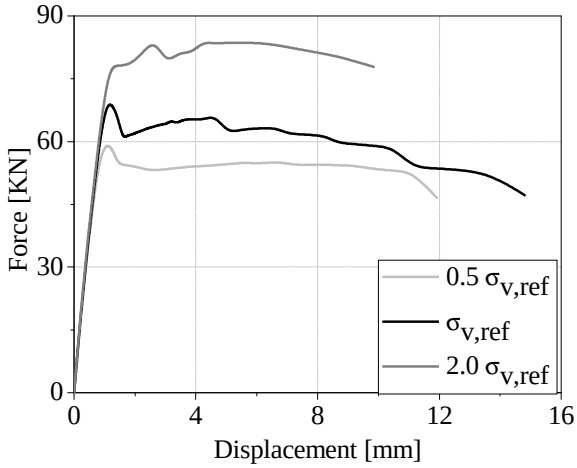

Figure 11 – Force-displacement curves for the parametric study of the pre-compression level.

4.4 Geometric parameters

Supplementary studies were also carried out in order to evaluate the influence of the geometric parameters on the behaviour of the anchoring system, as follows: steel bar diameter and respective borehole, wall width and embedment depth, and the spacing between anchors.

The steel bar diameter and corresponding borehole were studied in order to evaluate how the anchor dimensions can affect the behaviour of the system. A new model was created by modifying the anchor dimensions, the steel bar diameter (32 mm instead of 16 mm) and the corresponding borehole (75 mm instead of 50 mm). The parametric study showed that an increase of 100% in the anchor diameter (increase of 167% in perimeter) did not provide a significant increase in the ultimate capacity (around 11% regarding the reference model) (Figure 12a). The damage distribution is also very similar to the one found for the reference model as well as the non-linear behaviour of the model.

A study to evaluate the influence of the distance between the two anchors on the system behaviour was also conducted, aiming at evaluating changes in the ultimate capacity of the system and failure mode associated. A novel numerical model was prepared, in which the distance between the two anchors was increased from 280 mm to 420 mm, i.e. +50% of the initial distance. By comparing this model analysis with the reference, a slight increase in the ultimate capacity can be observed, see Figure 12b.

The maximum principal strains were also analysed as an indicator of damage in order to better understand the structural performance of the system. The damage in this analysis presents a different configuration between the two anchors where the cone formation is more visible. This analysis proved that the tensile capacity of a single anchor is affected by the overlapping of the adjacent anchors. This means that increasing the distance between anchors, up to an optimal minimum value, allows for the enhancement of the ultimate capacity of the system.

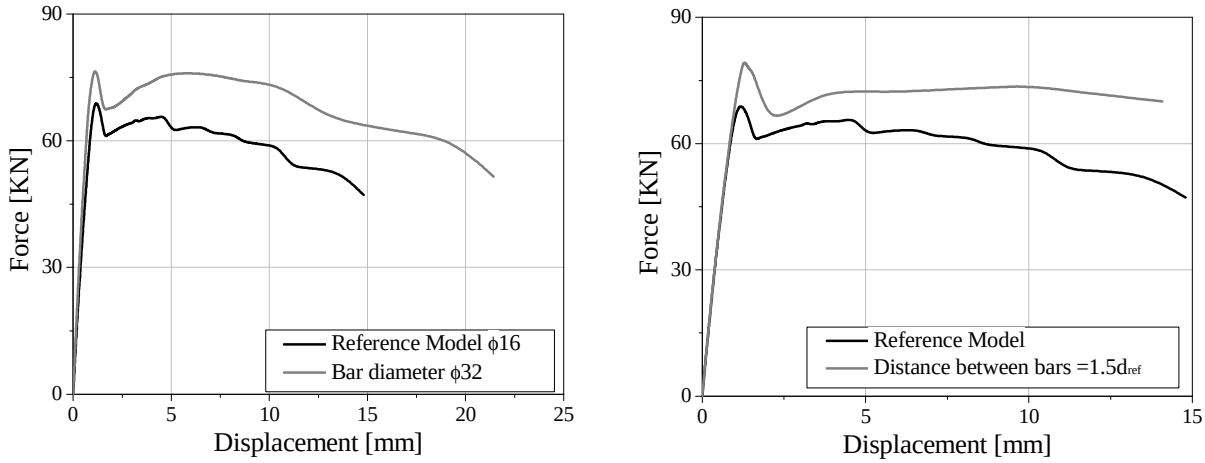

Figure 12 – Parametric studies: (a) Anchor diameter; (b) Anchors spacing.

According to several authors, the embedment depth of the anchor is a factor with great influence on the behaviour of the system. Hence, another numerical model was constructed by modifying the wall thickness from 400 to 600 mm and the embedment depth from 350 mm to 550 mm. The analysis results were compared to the reference model in Figure 13a where the differences on the behaviour of the models are apparent. The new model reaches a maximum force of 140 kN opposing to the 69 kN achieved by the reference model. Notwithstanding, the post-peak behaviour of the new model experiments a sharper decrease when compared to the reference model, which shows to be more ductile.

Figure 13b illustrates the maximum principal strains in the new model at failure, which can also be as an image of the tensile damage. This damage pattern presents significant differences regarding the one from the reference model, see Figure 8 for the RCM. The formation of the shear cone on the masonry is not activated for the whole anchor system extension as in the reference model, instead sliding along the external interface is perceptible until a certain position followed by the masonry cone development (visible in Figure 13b).

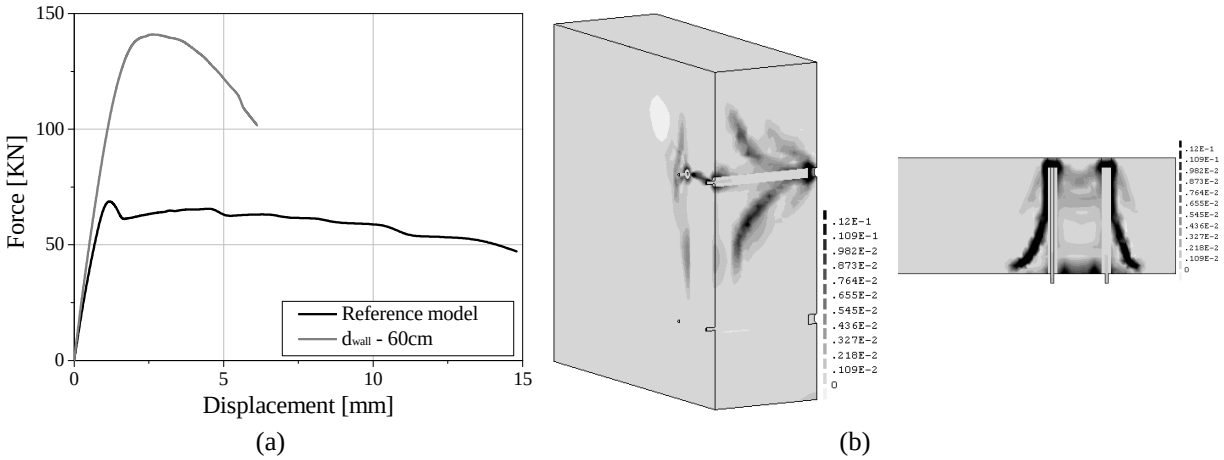

Figure 13 – Parametric study of the wall thickness and embedment depth: (a) Force-displacement curve; (b) Maximum principal strains at peak.

Overall, the parametrical studies showed that the parameter that most influences the structural behaviour of the system was the anchor embedment depth, as expected. The pre-compression level of the masonry, the anchor diameter and the spacing between anchors also influence the behaviour of the structural system although in a rather moderate extent.

5. ANALYTICAL EVALUATION

The assessment of the anchoring system capacity by means of complex numerical methods was relevant for a better understanding of the structural behaviour of the system. However, for design purposes, the use of simplified models is required. As mentioned before, despite the fact that injected anchors have been used for many years to strengthen masonry buildings, no generally methodology exists for the design of such anchoring systems.

During the last few decades several analytical models have been proposed to describe the behaviour of anchors in tension [7], [11], [15]–[17], [39]–[42]. In general the ultimate tensile load capacity is based on the simplified assumption of separated failure modes [30]. Moreover, some of the simplified analytical formulations presented in literature are adjusted to achieve a good fit with available test data.

This section reviews the most used simplified analytical methods, associated to distinct failure mechanisms occurring in injected anchors under tensile loading, and applies them to the example under study. Due to the few existing analytical formulations regarding anchors in masonry, formulations regarding anchors in concrete have also been employed. Most of these approaches are similar and the same parameters are recurrently used, such as: the embedment depth (l_{ef}), steel bar diameter (d_s) and area (A_s), borehole diameter (d_B), masonry compressive strength (f_m), anchor yield strength (f_y) and bond strength (τ_u). The symbol N will be used for the anchor capacity loaded in tension.

The analytical expressions provided by the Masonry Standards Joint Committee [42] to predict the anchor behaviour consider two failure mechanisms namely steel yielding or tensile breakout of masonry. Equation (1) is used to define the anchor capacity based on the steel yielding:

$$N = A_s \times f_y \tag{1}$$

The tensile breakout of masonry is computed using equations (2) and (3):

$$N = 0.332 \times A_{pt} \times \sqrt{f_m} \tag{2}$$

$$A_{pt} = \pi \times {l_{ef}}^2 - \frac{A_0}{2} \tag{3}$$

where A_0 is the overlapping area of the anchors. In the experimental tests under consideration f_y is equal to 640 MPa.

Based on the results of 500 pull-out tests performed in laboratory and in-situ, Gigla and Wenzel [11] proposed simplified expressions for ultimate capacity of anchoring systems. The bond strength between the grout and the surrounding masonry was also evaluated and Equation (4) proposed:

$$\tau_u = \emptyset_J \times \left(\frac{{f_{G,c}}^2}{500} + X_{B,W} \right) \tag{4}$$

where $\emptyset_J$ is the reduction factor for bed or head joints (assumed equal to 0.6), $f_{G,c}$ is the compressive strength of grout and $X_{B,W}$ is the term to describe the increase of bond strength inside water absorptive stone material (the recommended value is zero if the value is unknown).

As $f_{G,c}$ is equal to 51.5 MPa, the application of equation (4) gives a value for the bond strength around 3 MPa, which seems to be a reasonable value when compared with experimental studies [15], [18]. This value was also used in the formulations next, since no experimental values are available. The capacity of an injected anchor should be calculated using equation (5):

$$N = \tau_u \times \frac{A_B}{A_{g,d}} \times A_{A,d} \tag{5}$$

where τ_u is the bond strength , $A_{A,d}$ represents the surface of injected grout surrounding the steel bar, $A_{G,d}$ is the surface of injected grout and A_B is the contact area between grout and units (see Figure 14).

After the experimental tests carried out on the University of Minho, the walls were carefully demolished in order to assess the distribution of mortar and stone surrounding the grout surface. Considering the three experimental tests, an average value of 37% was found for the area of stone in contact with the grout surface, and a value of 63% for mortar (head and bed joints). With this information, a more realistic value for the contact area of grout and stone (A_B) was defined.

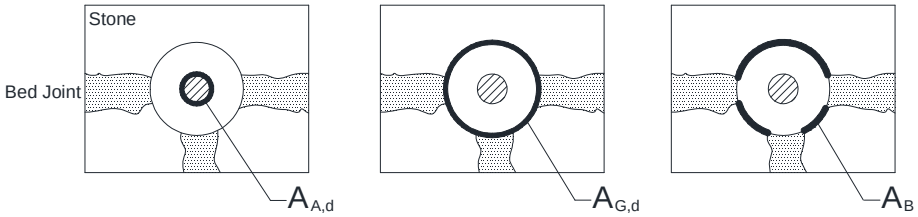

Figure 14 – Geometrical parameters for equation (16) [15].

The methodology proposed by ACI 318 Appendix D [39] for the prediction of the anchor strength in concrete defines three failure modes: steel tensile failure, substrate tensile breakout and bond failure. The design method proposed in Hilti [41] is based in this code. The strength of an anchor in tension governed by the steel is given by Equation (6):

$$N = n \times A_s \times f_{uta} \tag{6}$$

where n is the number of anchors in the group, and f_{uta} is the specified tensile strength of the anchor steel (equal to 800 MPa for the anchor under study). ACI 318 considers that the tension strength of anchors is best represented by f_{uta} rather than f_y because the large majority of anchor materials do not exhibit a well-defined yield point [39]. The base material breakout strength of anchors loaded in tension is defined as follows:

$$N = \frac{A_{Nc}}{A_{Nco}} \times \Psi_{ec,N} \times \Psi_{ed,N} \times \Psi_{c,N} \times \Psi_{cp,N} \times \ n \cdot N_b \tag{7}$$

$$A_{Nco} = 9 \times {l_{ef}}^2 \tag{8}$$

$$N_b = 4.10 \times \sqrt{f_m} \times {l_{ef}}^{1.5} \quad \text{[adapted for use in masonry [13]]} \tag{9}$$

where A_{Nc} is the projected failure area of a single anchor or group of anchors limited by the edge distance or spacing, as represented in Figure 15, $\Psi_{ec,N}$ is the modification factor for anchor groups loaded eccentrically, which is not the case under study so $\Psi_{ec,N}$ is equal to 1; $\Psi_{ed,N}$ is the modification factor for edge distances less than 1.5 l_{ef}, see equation (10), $\Psi_{c,N}$ is equal to 1.0 when the base material indicates cracking at service loads, which is considered to be case for masonry, and $\Psi_{cp,N}$ is the modification factor for splitting, equal to 1 in this case.

$$\Psi_{ed,N} = 0.7 + 0.3 \times \frac{c_a}{1.5\ l_{ef}} \quad if \ \ c_a < 1.5\ l_{ef} \tag{10}$$

According with the same methodology, the bond strength of adhesive anchor in tension is evaluated as follows:

$$N_a = \frac{A_{Na}}{A_{Nao}} \times \Psi_{ec,N_a} \times \Psi_{ed,N_a} \times \Psi_{cp,N_a} \times \ n \cdot N_{ba} \tag{11}$$

$$A_{Nao} = (2c_{Na})^2 \tag{12}$$

$$c_{Na} = 10 \cdot d_B \sqrt{\frac{\tau_u}{7.58}} \tag{13}$$

$$N_{ba} = \tau_u \times \pi \times d_B \times l_{ef} \tag{14}$$

where A_{Na} is the projected influence area of a single adhesive anchor or group, represented in Figure 15, and A_{Nao} is the projected influence area of a single anchor with an edge distance equal to c_{Na}

(obtained by the application of equation (13) with the constant 7.58 in N/mm^2), see equation (12). In this case the parameter Ψ_{ec,N_a} is equal to 1 since the anchor group is not eccentrically loaded. The modification factor for edge effects, Ψ_{ed,N_a}, is equal to 1 when $c_a > c_{Na}$, which is the case, and $\Psi_{cp,N_a}$the modification factor for splitting is also equal to 1.

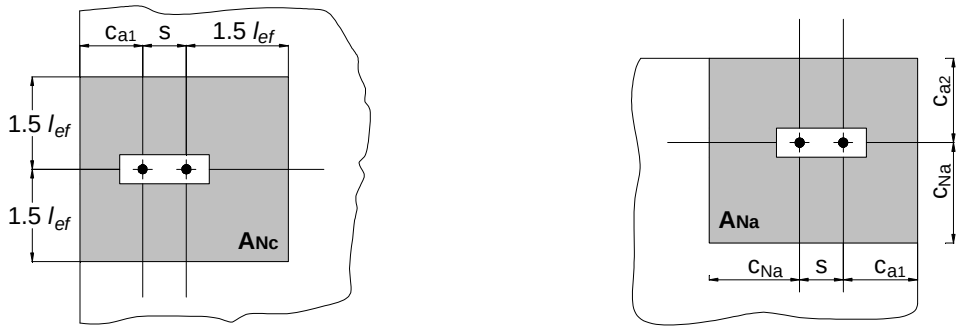

Figure 15 – Calculation of A_{Nc} and A_{Na} [39].

The analytical formulations recommended by ACI 318 for the substrate tensile failure and bond failure include the interaction between anchor groups. So, although the number of anchors n has been considered equal to 1 (in order to easily compare with the other predictions), the strength value obtained by the application of this formulation already takes into account the interaction between anchors.

CEB [43] proposes an approach to the design of anchors in concrete and masonry, where three failure modes are defined. For the definition of the capacity based on the steel failure equation (1) is used. As for the assessment capacity based on the base material cone failure the equation (15) is proposed by Eligehausen et al. [44]. Doerr and Klingner [45] present the equation (16) which attempts to incorporate the combined action of substrate-cone failure and bond failure.

$$N = 0.85 \times {l_{ef}}^2 \times \sqrt{f_m} \tag{15}$$

$$N = \frac{34.7\pi \times \tau_u \times {d_s}^{1.5}}{\lambda'} \times tanh\left[\frac{\lambda' \times \left(l_{ef} - 50\right)}{34.76 \times {d_s}^{0.5}}\right] \tag{16}$$

where λ' is a parameter that depends on the grout properties (see [45]), which equals 0.3 $mm^{-1/2}$ here. In the case of failure at the grout-masonry interface, the bond strength is smaller than the masonry strength. To take this failure mode into account, CEB proposes the following equation, also reported in D'Ayala [6] and Meyer and Eligehausen [16]:

$$N = \tau_u \times l_{ef} \times \pi \times d_B \tag{17}$$

The design guide for anchors in concrete available in fib Bulletin No. 58 [40] recommends the prediction of the anchor strength based on three failure modes. In addition, the strength of an anchor is evaluated by taking into consideration the interaction between anchors in a group. The anchor strength considering the steel failure is given by equation (6), as proposed by ACI 318. The combined pullout and substrate cone failure may be obtained as follows:

$$N_p = {N^0}_p \times \frac{A_p}{{A^0}_p} \times \Psi_{s,N_p} \times \Psi_{g,N_p} \times \Psi_{ec,N_p} \times \Psi_{re,N_p} \tag{18}$$

$${A^0}_p = \left(s_{cr,N_p}\right)^2 \tag{19}$$

$$s_{cr,N_p} = 20 d_s \sqrt{\frac{\tau_u}{7.5}} \tag{20}$$

$$c_{cr,N_p} = 0.5\, s_{cr,N_p} \tag{21}$$

where ${N^0}_p$ is computed using the equation (14) from ACI; ${A^0}_p$, the bond reference area, and A_p, actual bond influence area limited by overlapping areas of adjacent anchors, are calculated similarly to the method used in ACI 318 (see Figure 15). Ψ_{s,N_p} is a factor that takes into account the distribution of stresses due to the edges of the substrate member, equal to 1 in this case because $c > c_{cr,N_p}$ ($c = 380\ mm$). The factor Ψ_{g,N_p}, which takes into consideration the effect of the failure surface of anchor groups, and factor Ψ_{s,N_p}, which refers to non uniform tensile loads, are both equal to 1 in this study case (see [40]). The parameter that reduces the strength of anchors with embedment depth $l_{ef} < 100\ mm$ (Ψ_{re,N_p}) also takes the value of 1. The strength capacity in the case of the substrate cone failure is obtained from the following procedure:

$$N_c = {N^0}_c \times \frac{A_c}{{A^0}_c} \times \Psi_{s,N_c} \times \Psi_{ec,N_c} \times \Psi_{re,N_c} \tag{22}$$

$${A^0}_c = \left(s_{cr,N_c}\right)^2 \tag{23}$$

$$s_{cr,N_c} = 3l_{ef} \tag{24}$$

where ${N^0}_c$ is given by equation (9), the geometric factor $\frac{A_c}{{A^0}_c}$ is equal to the one used in ACI 318 for the same failure mode, see equation (7), as well as the Ψ_{s,N_c} factor given by equation (10). Ψ_{ec,N_c} and Ψ_{re,N_c} (already defined) are equal to 1.

Pull-out tests of single anchors in brick masonry were carried out by Arifpovic and Nielsen [17] with the purpose of observing the failure modes that govern the behaviour of the system in different conditions. Simplified analytical expressions based on the theory of plasticity were developed from the experimental results in order to predict the load carrying capacity of the anchors. Three failure modes were presented by the authors. The strength capacity of the anchor due to masonry cone failure can be obtained by equation (25):

$$N = 0.96(d_s + l_{ef}) \times l_{ef}\sqrt{{f'}_m} \tag{25}$$

For the case of bond failure, Arifpovic and Nielsen defined two expressions for the cases in which the anchor is installed in a mortar joint, equation (26), or in a unit, equation (27):

$$N = 22.38\sqrt{f_{cj} \times l_{ef}} \times {d_s}^{\frac{3}{2}} \tag{26}$$

$$N = 3.79 d_s \times l_{ef}\sqrt{f_{cb}} \tag{27}$$

where f_{cj} is the compressive strength of the mortar and f_{cb} represents the compressive strength of the unit. The compressive strength of the mortar and limestone units was experimental evaluated for the present case study and a mean value of 1.3 MPa and 107 MPa, respectively, was obtained. The combined brick-cone failure, which consists in the combination of the masonry cone formation and sliding along both the internal and external interface, can be obtained by equation (28):

$$N = [3.93\sqrt{f_{cb}} \times \left(l_{ef} - 5.76 \times d_s\right) \times d_s + 37.44\sqrt{f_{ci}} \times (l_u + d_s) \times d_s]\sqrt{\frac{d_s}{l_{ef}}} \tag{28}$$

where f_{ci} is the compressive strength of the interface between mortar and joints and l_u is the unit length. Here, a value around 0.3 MPa was adopted following the recommendations reported in the same report [17]. An average length (l_u) of 200 mm was considered taking into consideration the stone blocks used.

Figure 16 summarizes the different approaches considered to predict the anchor capacity, comparing these results to the mean experimental value. According to the experimental results, a mean force of 76.8 kN was reached for the two anchors composing the anchoring solution adopted. As the

formulations were used to predict the capacity of one anchor (including the interaction among groups when applicable), the obtained value is multiplied by two.

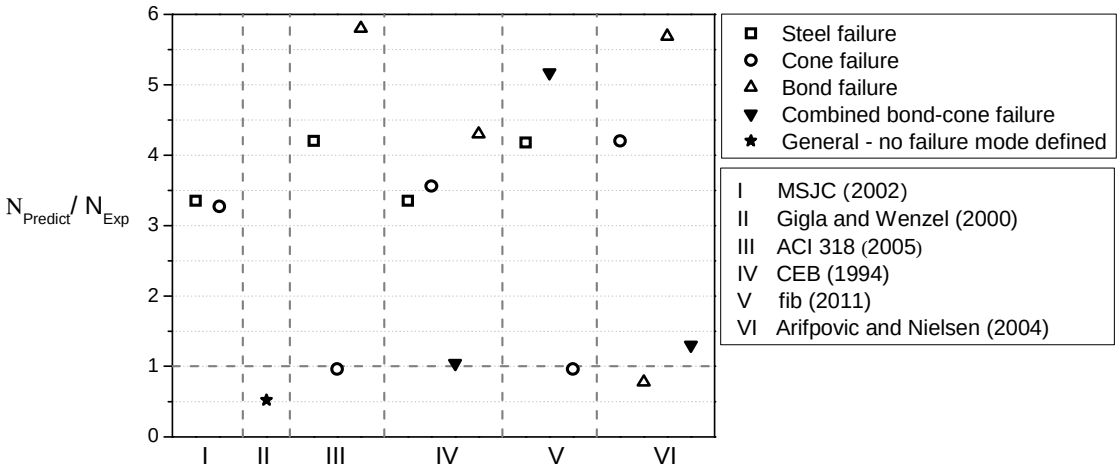

Figure 16 – Comparison between the experimental mean value and analytical predictions of the anchoring system capacity.

The prediction of the failure mode through simplified analytical methods appears to agree reasonably well with both the experimental results and numerical analysis. Either the base material cone formation with masonry breakout or the combined bond-cone failure are the recurrent failure modes, achieved in almost all the approaches. MSJC [42], ACI 318 [39], CEB [43] and fib bulletin 58 [40] predict that the anchor strength is limited by one of these failure modes. Arifpovic and Nielsen [17] predict the sliding of the anchor installed in a mortar joint as the failure mode limiting the anchor capacity (see Figure 16). However, the assumptions made in this study for this expression are not valid since the anchor is not completely installed in a mortar joint, therefore the corresponding value found is not applicable. Disregarding this value, the failure mode obtained by this formulation is the combined masonry cone formation with sliding along the interface. Gigla and Wenzel [11] do not define a specific failure mode.

The relations presented in Figure 16 show that the predicted strength values by ACI 318 and fib bulletin 58 for the masonry cone failure, and by Doerr and Klingner [45] for the combined bond-cone failure, are in very good agreement with the experiments. The good predictions of these two formulations, regarding both the failure mode and the strength value, can be explained by some considerations included in the expressions that are important in the anchoring system under study. Besides MSJC provisions, ACI 318 code and fib are the only that consider the influence of the anchors spacing and possible interaction among them. The formulation provided by Doerr and Klingner in CEB includes the prediction of a combined failure mode (masonry cone with sliding along the interface) that was verified experimentally. The expression provided by Gigla and Wenzel [11] predicted very conservative relations.

As expected, the applied analytical formulations based on the steel failure and bond failure achieve considerably high tensile load capacities. The analytical formulation defined by fib bulletin 58 for the combined bond-cone failure also resulted in a high strength value. When compared with other formulations, this analytical expression seems to be more appropriate to define the bond failure. Finally, the simplified approach recommended by MSJC gives a very high value when compared to experiments, and even with the other simplified expressions. Weigel and Lyvers [13] have stated that these provisions may lead to less reliable results.

6. FINAL CONSIDERATIONS

A possible strengthening solution to improve the seismic response of masonry-to-timber connections in masonry constructions was assessed. A numerical study was made here, based on the experimental campaign carried out at the University of Minho, with the purpose of evaluating the structural behaviour of injected anchors in masonry.

A detailed numerical model was prepared in accordance with the experimental setup, using a macro-modelling technique for the masonry wall. The model was calibrated and validated in accordance to the available experimental results. Both the fixed and rotating crack formulations were applied and evaluated by comparing the analysis results with experiments. The rotating crack model (RCM) showed a better agreement regarding the post-peak behaviour since the shear strength is updated after cracking along the complete analysis. When compared to the experimental results, the numerical analysis shows a good agreement both in terms of initial stiffness, strength and failure mode.

Parametric analyses were carried out in order to assess how the material parameters, wall pre-compression level and geometrical conditions influence the anchoring system behaviour. In the overview of the sensitivity analysis results, the embedment depth proved to be the parameter that most strongly influences the capacity of the anchoring system. The compressive strength and tensile parameters also influence the capacity and behaviour of the system although moderately. The pre-compression level proved to be a parameter that influences the behaviour of the system to some extent.

Available simplified formulations for the evaluation of the anchor tensile strength were discussed and applied to the case study. A good agreement between the experimental and the predicted failure mode by all the simplified models was attained. In terms of strength capacity, a very good agreement was obtained with the ACI 318 [39], fib bulletin 58 [40] and CEB [43] formulations. On the other hand, the method proposed by MSJC [42] seems to greatly overestimate the values of the strength capacity.

7. ACKNOWLEDGEMENTS

This work was partly funded by project FP7-ENV-2009-1-244123-NIKER. The first author also acknowledges the financial support from the Portuguese Science Foundation (Fundação de Ciência e Tecnologia, FCT), through grant SFRH/BD/71599/2010.

8. REFERENCES

[1] G. Vasconcelos, “Experimental investigations on the mechanics of stone masonry: Characterization of granites and behavior of ancient masonry shear walls,” Universidade do Minho, 2005.

[2] A. Mandara, F. Ramundo, and G. Spina, “Performance levels under seismic actions of masonry structures retrofitted with steel elements,” *Protection of Historical Buildings - PROHITECH 09*, pp. 1045–1050, 2009.

[3] I. Senaldi, G. Magenes, and J. M. Ingham, “The seismic performance of unreinforced stone masonry buildings during the 2010-2011 Canterbury earthquake sequence,” in *15th World Conference on Earthquake Engineering*, 2012, no. April.

[4] P. B. Lourenço, N. Mendes, L. F. Ramos, and D. V Oliveira, “Analysis of Masonry Structures Without Box Behavior,” *International Journal of Architectural Heritage*, vol. 5, no. 4–5, pp. 369–382, Jul. 2011.

[5] P. B. Lourenço, N. Mendes, and R. Marques, “Earthquake Design and Assessment of Masonry Structures : Review and Applications,” *20th International conference on Civil, Structural and Environmental Engineering Computing*, pp. 1–24, 2009.

[6] D. D. Ayala, “The role of connections in the seismic resilience of historic masonry structures,” in *XIV Convegno ANIDIS “L’Ingegneria Sismica in Italia,”* 2011.

[7] F. Wenzel and H. Maus, “Repair of Masonry Structures,” *Meccanica*, vol. 27, no. 3, pp. 223–232, 1992.

[8] D. D’Ayala and S. Paganoni, “Testing and design protocol of dissipative devices for out-of-plane damage,” *Proceedings of the Institution of Civil …*, pp. 167, 26–40., 2014.

[9] C. Modena, F. Da Porto, F. Casarin, M. Marco, and S. Elena, “Cultural Heritage Buildings and the Abruzzo Earthquake: Performance and Post- Earthquake Actions,” *Advanced Materials Research*, vol. 133–134, pp. 623–628, 2010.

[10] G. Magenes, “Masonry Building Design in Seismic Areas: Recent Experiences and Prospects from a European Standpoint,” in *1st European Conference on Earthquake Engineering and Seismology*, 2006, no. September, pp. 1–22.

[11] B. Gigla and F. Wenzel, “Design Recommendations For Injection Anchors As Supplementary Reinforcement Of Historic Masonry,” in *12th International Brick/Block Masonry Conference*, 2000, pp. 691–706.

[12] W. M. McGinley, “Design of anchor bolts in masonry,” *Progress in Structural Engineering and Materials*, vol. 8, no. 4, pp. 155–164, 2006.

[13] T. A. Weigel and G. Lyvers, “Statistical Analysis of Masonry Fastners,” in *13th International Brick and Block Conference*, 2004, pp. 89–98.

[14] A. Haman and W. Jaeger, “Experimental Investigation of Grouted Anchors in Natural Stone Masonry Walls under Static and Cyclic Loading,” in *9th Australasian Masonry Conference*, 2011, pp. 41–50.

[15] B. Gigla, “Bond Strength of Injection Anchors as Supplementary Reinforcement Inside Historic Masonry,” in *13th International Brick and Block Conference*, 2004, pp. 119–128.

[16] A. Meyer and R. Eligehausen, “Injection Anchors for use in Masonry Structures,” in *13th International Brick and Block Conference*, 2004, pp. 109–117.

[17] F. Arifpovic, M. P. Nielsen, and F. Arifovi, “Strength of anchors in masonry,” 2004.

[18] C. Algeri, E. Poverello, G. Plizzari, and E. Giuriani, “Experimental Study On The Injected Anchors Behaviour On Historical Masonry,” *Advanced Materials Research*, vol. 133–134, pp. 423–428, 2010.

[19] D. Dizhur, A. Schultz, and J. M. Ingham, “Performance of adhesive wall-to-diaphragm connections in the Canterbury earthquakes and the subsequent experimental pull-out test program,” in *12th Canadian …*, 2013.

[20] A. F. Ashour and M. A. Alqedra, “Concrete breakout strength of single anchors in tension using neural networks,” *Advances in Engineering Software*, vol. 36, no. 2, pp. 87–97, Feb. 2005.

[21] A. Haman and W. Jaeger, “Experimental Investigation of Grouted Anchors in Natural Stone Masonry Walls under Static and Cyclic Loading,” in *9th Australasian Masonry Conference*, 2011, pp. 41–50.

[22] S. Moreira, L. F. Ramos, D. V Oliveira, R. P. Fernandes, J. Guerreiro, and P. B. Lourenço, “Experimental seismic behaviour of wall-to-half-timbered wall connections,” in *8th International Conference on Structural Analysis of Historical Constructions*, 2012.

[23] V. Cóias, *Reabilitação Estrutural de Edifícios Antigos*. Lisboa: GECoRPA, 2007, pp. 1–4.

[24] DIANA 9.4, “DIANA, DIsplacement method ANAlyser, release 9.4, User’s Manual.” 2009.

[25] P. B. Lourenço, G. Milani, A. Tralli, and A. Zucchini, “Analysis of masonry structures: review of and recent trends in homogenization techniques,” *Canadian Journal of Civil Engineering*, vol. 34, no. 11, pp. 1443–1457, Nov. 2007.

[26] L. N. Lowes, “Finite Element Modeling of Reinforced Concrete Beam-Column Bridge Connections,” University of California, Berkeley, 1999.

[27] X. Q. Zhu and S. S. Law, “Damage detection of reinforced concrete structures based on concrete-steel interface element,” in *IMAC-XXIII: Conference & Exposition on Structural Dynamics - Structural Health Monitoring*, 2005, no. 1999.

[28] Y.-H. Lee, Y. T. Joo, T. Lee, and D.-H. Ha, “Mechanical properties of constitutive parameters in steel–concrete interface,” *Engineering Structures*, vol. 33, no. 4, pp. 1277–1290, Apr. 2011.

[29] Y. J. Jeong, H. Y. Kim, H. B. Koo, and S. T. Kim, “Steel-concrete interface behavior and analysis for push-out,” *KSCE Journal of Civil Engineering*, vol. 9, no. 2, pp. 119–124, Mar. 2005.

[30] M. Bajer and J. Barnat, “The glue–concrete interface of bonded anchors,” *Construction and Building Materials*, vol. 34, pp. 267–274, Sep. 2012.

[31] P. B. Lourenço, “A user / programmer guide for the micro-modeling of masonry structures,” no. 03, pp. 1–46, 1996.

[32] P. B. Lourenço, “Analysis of Masonry Structures with Interface Elements Theory and Applications,” *Delft University of Techonology*, no. 03, pp. 1–25, 1994.

[33] D. Jarred and C. Haberfield, “Tendon/Grout Interface Performance in Grouted Anchors,” in *Ground anchorages and anchored structures*, G. S. Littlejohn, Ed. London, U.K.: Tomas Telford, 1997, pp. 3–12.

[34] S. Eshghi and K. Pourazin, “In-plane Behaviour of Confined Masonry Walls - With and Without Opening,” *International Journal of Civil Engineering*, vol. 7, no. 1, pp. 49–60, 2009.

[35] D. V Oliveira, “Experimental and numerical analysis of blocky masonry structures under cyclic loading,” University of Minho, 2003.

[36] J. G. Rots, “Computational Modeling of Concrete Fracture,” *PhD Thesis*, 1988.

[37] P. B. Lourenço, “Recent Advances in Masonry Modelling: Micromodelling and Homogenisation,” in *Multiscale Modeling In Solid Mechanics Computational Approaches*, Imperial C., U. Galvanetto and M. H. Aliabadi, Eds. Imperial College Press, 2009, pp. 251–294.

[38] P. B. Lourenço, “Slides from SAHC - Material Data to Use,” in *SAHC*, 2009.

[39] ACI 318, *Building Code Requirements for Structural Concrete (ACI 318-11) and Commentary*. 2011.

[40] fib Bulletin No. 58, *Design of anchorages in concrete: Guide to Good Practice*. 2011.

[41] Hilti, “North American Product Technical Guide - Volume 2: Anchor Fastening Technical Guide,” 2011.

[42] MSJC - Masonry Standard Joint Committee’s, *Building Code Requirements for Masonry Structures (TMS 402-13/ ACI 530-13/ ASCE 5-13)*. 2013, pp. 125–128.

[43] CEB, *Fastenings to Concrete and Masonry Structures*. Comite Euro-International du Beton, 1994.

[44] R. Eligehausen, R. Mallée, and G. Rehm, “Befestigungen mit Verbundankern (Fastenings with bonded anchors),” *Betonwrk + Fertigteil-Technik*, no. No.10, 682–692. No.11, 781–785. No. 12, 825–829, 1984.

[45] G. T. Doerr and R. E. Klingner, “Adhesive Anchors: Behavior and Spacing Requirements,” Austin, Texas, 1989.

List of Figures:

List of Tables: